Individual Phase Flow Rate Measurement Technique Using Optical Fiber Sensor in Horizontal Stratified Flow

Hanna Kim, Rira Park, Hyungmo Kim*
Gyeongsang National University, Department of Mechanical Engineering
501 Jinju-daero, 52828, Jinu, Republic of Korea
hanna36@gnu.ac.kr, baglila4089@naver.com, hyugnmo@gnu.ac.kr*

ABSTRACT

Traditional flow meters, such as orifice and venturi meters, are effective for total flow measurement but have limitations in precisely identifying the phase distribution across a pipe's cross-section in two-phase flows like stratified flow. Consequently, this study proposes a technique using a distributed optical fiber sensor to identify phase distribution and measure individual phase flow rates. The proposed method identifies the air-water interface and flow velocity through temperature profiles obtained from the optical fiber sensor, utilizing this information for individual flow rate calculation. Specifically, the interface is identified based on temperature characteristic changes resulting from heat capacity differences between water and air, while the velocity is calculated via differences in temperature profiles caused by variations in convective heat transfer. To validate this, a horizontal pipe experimental setup simulating water-air stratified flow was developed. A sensor with a spatial resolution of 0.65 mm and a sampling rate of 15.61 Hz was inserted vertically, securing temperature data from 148 measurement points. Experiments were conducted with water flow rates up to 13 L/min and air flow rates up to 55 L/min to cover laminar, transitional, and turbulent regimes. The analysis results showed that the interface heigh could be successfully identified through distinct temperature gradient changes at the air-water interface. Furthermore, it was confirmed that the maximum temperature difference in a quasi-equilibrium state varies due to differences in the convective heat transfer rate corresponding to velocity changes, validating its potential as a velocity identification index. This study experimentally verified the proposed measurement concept and suggests practical applications for individual phase flow measurement in stratified flows.

Keywords: *Distributed temperature sensing, Rayleigh backscattering, Interface measurement, Flow velocity measurement, Air-water stratified flow*

1 INTRODUCTION

Steam piping in the secondary system of nuclear power plants is designed to maintain single-phase flow under high-pressure and high-temperature conditions during normal operation. However, in actual operational environments, two-phase flow, where steam and water coexist, can occur due to various factors [1]. Specifically, changes in flow conditions arise during transient states such as power ramps or lower-power operations, while phase changes caused by pressure drops and heat loss in long-distance pipelines lead to the formation of multiphase flows, such as stratified flow. In such environments, identifying individual phase flow rates is essential for accurately analyzing thermo-hydraulic behavior and ensuring operational reliability. Conventional differential pressure-based instruments, such as Venturi and orifice flow meters, face technical limitations in two-phase flow conditions, as the correlation between pressure drop and flow rate becomes distorted due to density differences between steam and liquid and complex interfacial friction [2-4]. Furthermore, these existing devices are restricted to point-based measurements and cannot provide comprehensive phase

distribution information across the pipe's cross-section. Alternative hardware-based devices often involve high costs, strict management procedures for radioactive sources, or significant consumption of resources and time for phase separation [5].

To overcome these limitations, this study proposes a measurement technique using distributed optical fiber sensors to identify cross-sectional phase distribution and measure individual phase flow rates. As a preliminary evaluation prior to application in actual steam-water environments, experiments were conducted within an air-water stratified flow environment to verify the validity of the proposed concept. The technique identifies the phase interface based on heat capacity differences between water and air, while flow velocity is determined by analyzing convective heat transfer variations reflected in high-resolution temperature profiles [6-9]. For this purpose, a horizontal pipe experimental setup was developed to simulate diverse flow regimes, ranging from laminar to turbulent flows. By integrating a high-resolution distributed optical fiber sensor into the test section, continuous temperature data were acquired across the pipe cross-section, enabling a more comprehensive analysis of phase distribution compared to point-based sensors. This study focuses on validating the measurement principle and identifying key physical indicators derived from thermal profiles that characterize each phase parameter. Ultimately, these findings provide experimental evidence to support the development of advanced flow monitoring systems for nuclear secondary circuits.

2 MEASUREMENT METHOD

2.1 Distributed Optical Fiber Sensor

In this study, the distributed optical fiber sensor used enables continuous measurement of physical parameters such as temperature and strain along the entire length of an optical fiber, providing multi-point sensing capability with a single fiber. A polyimide-coated temperature sensing fiber (LUNA Inc.) was employed and interrogated using the LUNA ODiSI 6100 system. This system operates based on Rayleigh scattering through Optical Frequency Domain Reflectometry (OFDR), in which the input laser wavelength is continuously swept through the fiber and position-dependent variations in the Rayleigh backscattered signal induced by temperature changes are analyzed, as shown in Fig. 1 [10-14]. This system provides a spatial resolution of 0.65 mm and a sampling rate of 15.61 Hz. As a result, this configuration allows real-time, spatially continuous temperature measurement along the entire fiber length. Compared to conventional point-type sensors, the distributed optical fiber sensor offers several advantages, including spatially continuous monitoring with a single fiber, minimal disturbance to the flow, and immunity to electromagnetic interference [15-16].

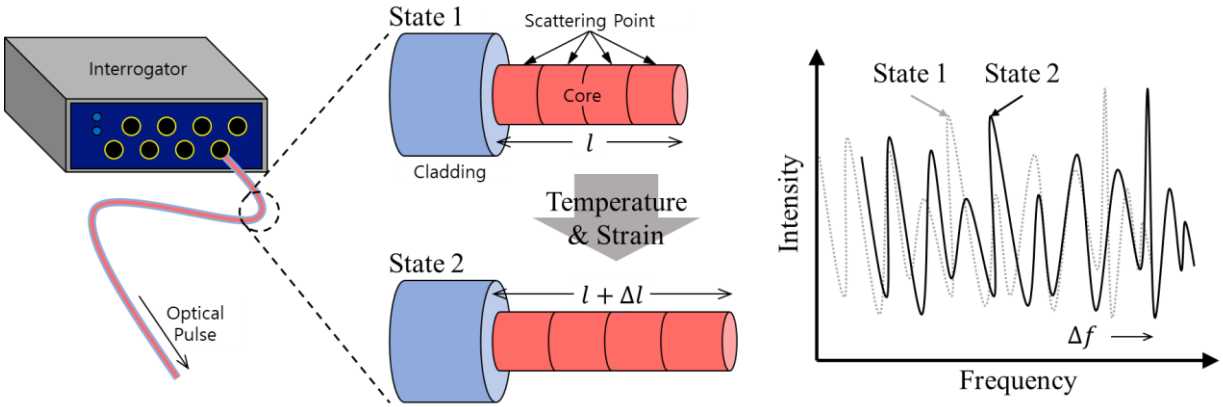

Figure 1: Measurement principles of Rayleigh scattering-based sensor using OFDR

2.2 Principles of Individual Phase Flow Rate Estimation

The fundamental principle for calculating the individual flow rates of gas and liquid phases under stratified flow conditions lies in the integration of the fluids' geometric distribution and kinematic characteristics. As defined in Eq. (1), the volumetric flow rate (Q) for a specific phase is determined by the product of the pipe cross-sectional area (A) occupied by the fluid and its average flow velocity ($\bar{v}$)

$$Q = A \times \bar{v} \tag{1}$$

The measurement technique proposed in this study involves applying a consistent amount of thermal energy via Joule heating to a stainless steel (STS) tube containing a distributed optical fiber sensor, followed by a real-time analysis of the induced temperature profiles. As the applied heat is transferred from the tube surface to the surrounding fluid, the temperature distribution captured by the internal sensor is dictated by the thermophysical properties and flow conditions of the fluid. The physical mechanisms for deriving the across-sectional area and flow velocity from these thermal responses are detailed as follows.

First, the identification of the phase interface for calculating the cross-sectional area (A) exploits the differences, specifically volumetric heat capacity (ρC_p) and thermal diffusivity (α). Since water possesses a significantly greater capacity to absorb and diffuse heat compared to air, it maintains a lower temperature and exhibits more stable thermal behavior upon contact with the heated tube. These contrasting physical properties create a distinct inflection point in the temperature gradient at the boundary where the liquid and gas phases meet. By tracking this point through distributed optical fiber sensor data, the interface level (h) and the resulting phase-occupied cross-sectional area (A) can be precisely determined.

The calculation of flow velocity ($\bar{v}$) is based on the mechanism of convective heat transfer between the heated tube and the flowing fluid. The convective heat transfer coefficient (h_c), which dictates the rate of heat transfer from the tube surface to the fluid, is intrinsically linked to the fluid's velocity. Variations in flow velocity lead to differences in the amount of heat loss from the tube surface. In a quasi-equilibrium state, where the supplied thermal energy and the energy lost through convection reach a thermal balance, changes in velocity are directly reflected in the local temperature behavior measured by the sensor. The proposed technique quantitatively derives flow information for each phase by analyzing these temperature variation characteristics under thermodynamic equilibrium. A conceptual schematic of these measurement principles is illustrated in Fig. 2. Through this integrated approach, comprehensive cross-sectional flow information-which has been difficult to obtain with conventional point-based sensors-can be processed to quantify individual phase flow rates.

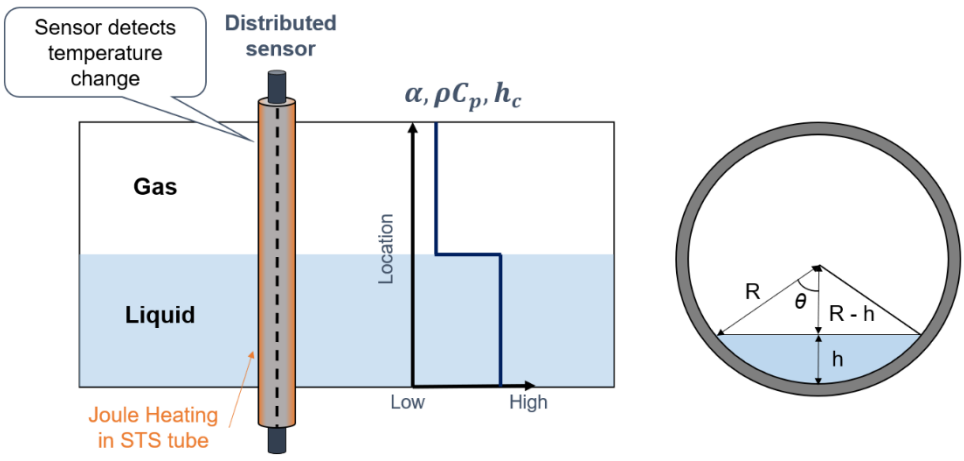

Figure 2: Physical principles of individual phase flow estimation

3 EXPERIMENT AND RESULTS

3.1 Experimental System

To verify the experimental validity of the proposed measurement technique, a horizontal pipe experimental setup was developed for a preliminary evaluation simulating an air-water stratified flow environment. The overall schematic of the experimental system is shown in Fig.3. The test section was established within a horizontal pipe, where a optical fiber sensor was inserted into a STS tube positioned vertically relative to the flow direction. This vertical installation allows the sensor to continuously monitor the temperature across the entire cross-sectional area of the pipe. The sensor was encased in the STS tube specifically to eliminate signal interface from mechanical strain and to provide physical protection. To ensure rapid thermal response and minimize measurement delays caused by thermal resistance, the tube was with a minimal internal gap relative to the fiber. Furthermore, the thickness of the STS tube was minimized to mitigate any disturbances to the flow tield within the test section. The optical fiber sensor utilized in this work provides a high spatial resolution of 0.65 mm, enabling the acquisition of temperature data from 148 measurement points across the 9.6 cm inner diameter pipe. With a sampling rate of 15.61 Hz, the system effectively captures thermal response of the fluid.

The experimental loop was designed to simulate diverse flow conditions, ranging from laminar to turbulent flows. In this configuration, water is operated in a circulation loop via a pump, while air follows a once-through path, entering from an external supply and being discharged after passing through the test section. The flow rates were controlled up to 13 L/min the test section. The flow rates were controlled up to 13 L/min for water and 55 L/min for air, ensuring a robust experimental foundation for evaluating the feasibility of individual phase flow quantification in stratified flow environments.

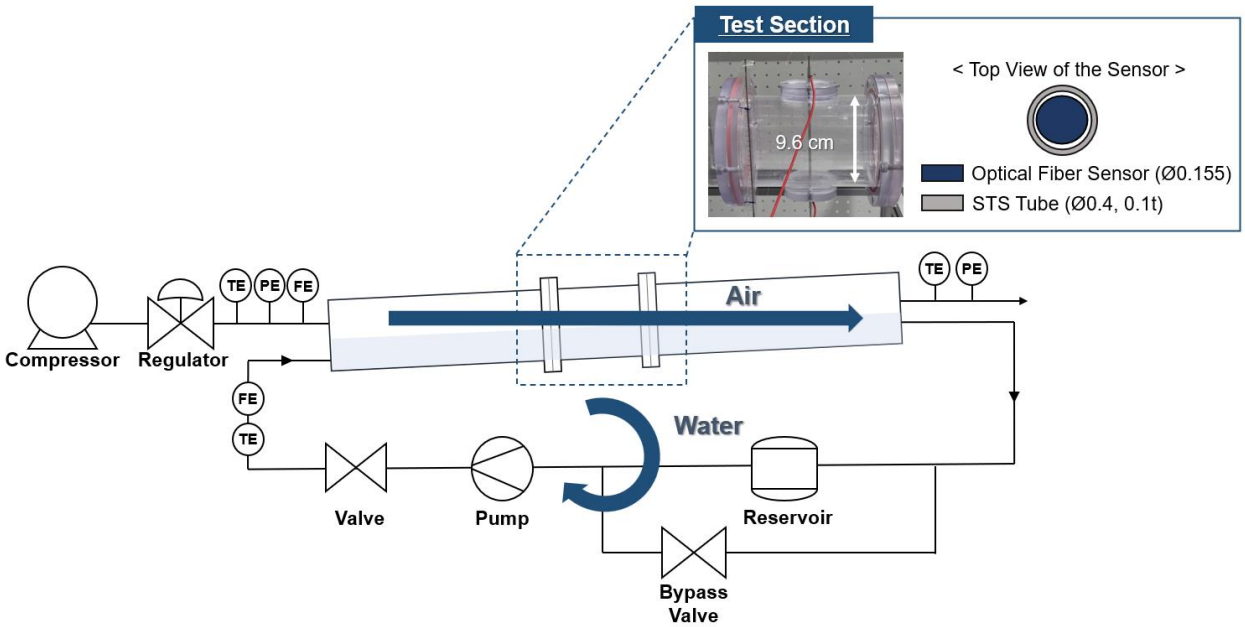

Figure 3: Schematic of the experimental system for air-water stratified flow

3.2 Experimental Verification of Interface Measurement

Experiments for interface verification were conducted to evaluate whether the proposed concept can effectively detect phase interfaces and provide indicators for estimating the cross-sectional area. The experiments were performed under laminar flow conditions for both water and gas phases, measurements were initiated only after establishing a steady state where flow rates and interfaces

remained constant. A constant heat flux of 25 kW/m² was supplied via Joule heating, while the optical fiber sensor simultaneously recorded the temperature distribution across the entire 9.6 cm flow region within the pipe, as shown in Fig. 4(a). In the data preprocessing stage, a 15-sample moving average was applied to the raw data to mitigate noise. To establish a consistent reference, all measured data were baseline-corrected by aligning them to the initial temperature profile recorded at the moment of measurement initiation. Based on this normalized baseline, the relative temperature change induced by heating, ΔT(t,z), was determined by subtracting the temperature profile at the onset of heating (t=0) from the data at any given time t , as defined in Eq. (2).

$$\Delta T(t,z) = T(t,z) - T(0,z) \quad (2)$$

Fig. 4(b) shows the temperature change profile derived using Eq. (2) at 5 seconds after heating initiation, T(5,z), where the x-axis represents the temperature difference (ΔT) and the y-axis indicates the location within the pipe. As discussed in Section 2.2, the profile exhibited distinct differentiation between phases due to differences in volumetric heat capacity and thermal inertia. Critically, the sharp gradient region in the data coincided with the observed interface point from the experiment, validating that the gradient inflection point serves as a robust physical indicator for determining the phase-occupied across sectional area.

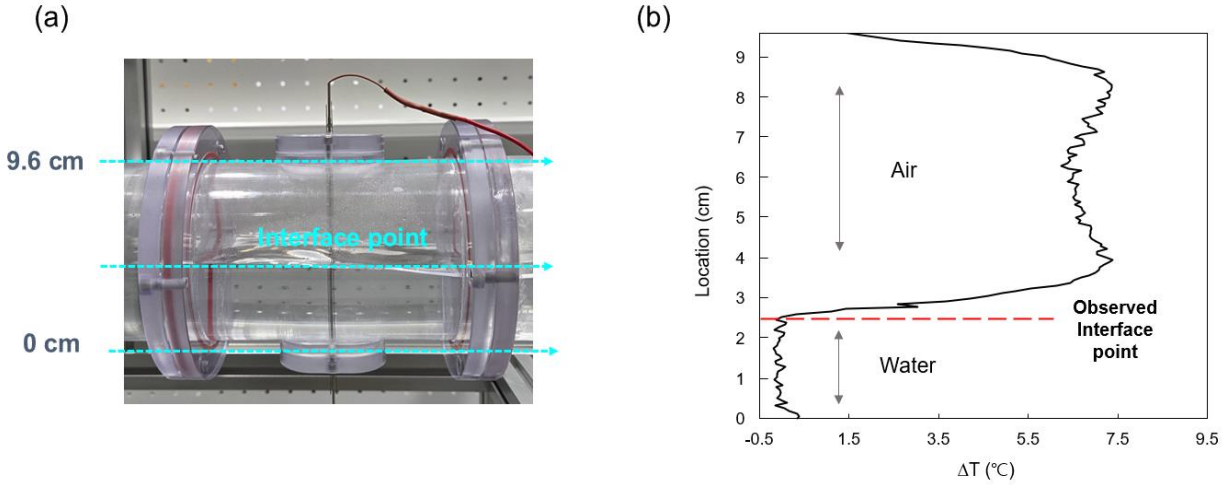

Figure 4: (a)Sensor arrangement within the pipe, (b)Temperature profile after 5 seconds of heating

However, continuous heating exhibited limitations for long-term interface monitoring due to cumulative system heat losses. As illustrated in Fig. 5(a), the temperature change profiles evaluated at successive time intervals (ΔT_1, ΔT_2, ΔT_3) show a gradual reduction in the inter-phase temperature difference. This behavior across the system, diminishing the distinct thermal inertia effects described in Section 2.2 and complicating interface estimation based on temperature gradients.

To address this limitation, the validity of the interface indicator was investigated under cooling conditions, established by turning the power supply off. As shown in Fig. 5(b), Eq. (2) was applied 15 seconds after the initiation of both heating (power on) and cooling (power off) phases respectively. The results demonstrate that the sharp temperature gradient at the interface remains clearly identifiable even during the cooling state where power is removed. Critically, this gradient inflection point coincided with the observed interface point from the experiment. In conclusion, these findings prove that periodic heating and cooling cycles enable more stable and sustainable long-term interface monitoring in heat loss prone environments. This intermittent approach not only prevents sensor overheating to enhance system stability but also ensures the continuous acquisition of cross-sectional area data for individual phase flow quantification.

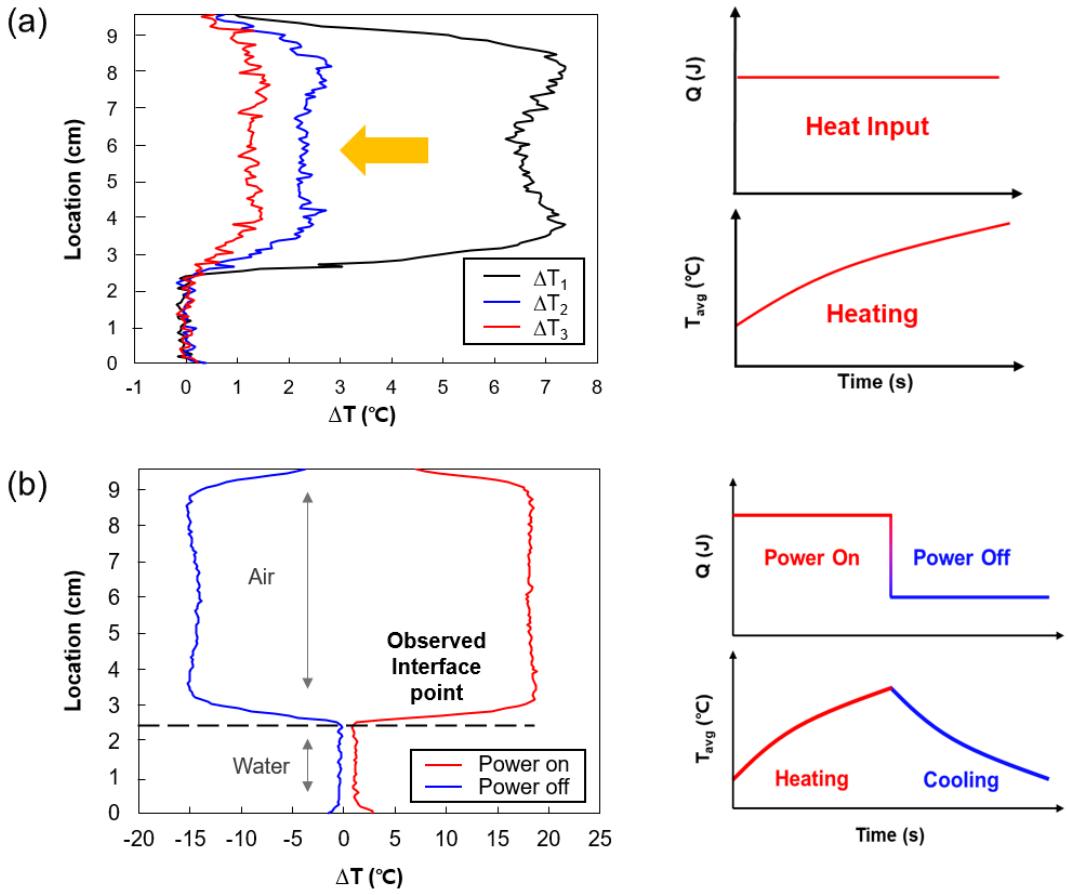

Figure 5: (a)Convergence of temperature profiles under continuous heating and system heat loss, (b)Validation of interface identification indicators during heating and cooling cycles

3.3 Experimental Verification of Flow Velocity Measurement

To verify the experimental validity of the flow velocity measurement technique, the thermal response characteristics of each phase were analyzed by conducting a series of independent experiments at various constant flow rate settings while applying a constant heat flux of 25 kW/m², identical to the interface identification tests. The reference flow rate data for each experimental case were obtained from flow meters installed at the inlet of each fluid (water and air). Under the air-water stratified flow conditions, the gas and liquid phases coexist within the pipe, and the interface level fluctuated depending on the specific flow rate combinations. To account for these variations, the minimum and maximum interface heights were recorded for each case, and their arithmetic mean was used as the reference interface to calculate the average flow velocity for each phase. These phase-specific velocity changes were isolated and analyzed separately. The detailed experimental conditions and flow ranges for each case are summarized in Table 1.

Table 1: Experimental conditions

No.	Average Velocity [cm/s]		Re		Liquid Level [cm]
	Water	Air	Water	Air	
1	0.46	7.1	248	1144	2.3
2	3.87	10.5	2756	1246	3.1 ~ 3.2
3	5.31	18.2	4046	1995	3.3 ~ 3.5
4	6.53	17.0	5453	1673	3.5 ~ 4
5	5.82	19.5	4710	2192	3 ~ 4

In the data preprocessing stage, a 15-sample moving average was applied to the raw data sampled at 15.61 Hz to mitigate signal noise. Consistent with the previously described procedure, all measured data were baseline-normalized by aligning them to the initial temperature profile at the moment of measurement initiation. To quantify the representative thermal response of each phase, a 1 cm vertical observation window was established at the center of each phase region. Within this domain, the spatially averaged temperature change over time, denoted as $\bar{T}_{avg,1cm}(t)$, was extracted as a time-series dataset. The central region was specifically selected for observation because the pipe's velocity profile typically exhibits its peak sensitivity to flow variations at the center. Furthermore, this localized averaging approach effectively minimizes potential interference from wall effects or interface fluctuations, thereby ensuring a robust correlation between the thermal response and the flow velocity.

The experimental results for the liquid phase (water), presented in Fig. 6(a), demonstrated that the average temperature reached in a quasi-equilibrium state decreased as the flow velocity increased. This trend is consistent with the convective heat transfer mechanism discussed in Section 2.2, higher flow velocities enhance the convective heat transfer coefficient at the heated tube surface, thereby increasing the heat loss from the sensor to the fluid. Consequently, the thermodynamic balance between the supplied thermal energy and the dissipated energy is established at a lower temperature. This inverse relationship serves as a fundamental physical basis for quantitative flow estimation. In contrast, for the gas phase (air), certain experimental cases initially exhibited deviations from theoretical predictions, as shown in Fig. 6(b).

To investigate these discrepancies, the initial temperature fluctuations of the inlet fluid were analyzed and are summarized in Table 2. The results revealed that the inconsistencies were directly linked to the thermal stability of the incoming flow. Specifically, in Gas Case 4, the initial temperature fluctuation was relatively large (about 0.5°C), which impaired the correlation with velocity. Conversely, in cases where the fluctuation was maintained below 0.2°C, a reliable trend was observed. Even for the liquid phase, the velocity-temperature correlation became more pronounced when the initial fluctuation remained within 0.25°C (Table 2). By filtering the gas phase data based on this thermal stability criterion (fluctuation < 0.2°C), a consistent and reliable flow-temperature correlation was successfully secured, as depicted in Fig. 7. These findings suggest that instability in the inlet temperature can induce errors in the baseline setting, thereby affecting experimental consistency. Thus, maintaining a constant inlet fluid temperature is identified as a critical technical requirement for high-reliability measurements.

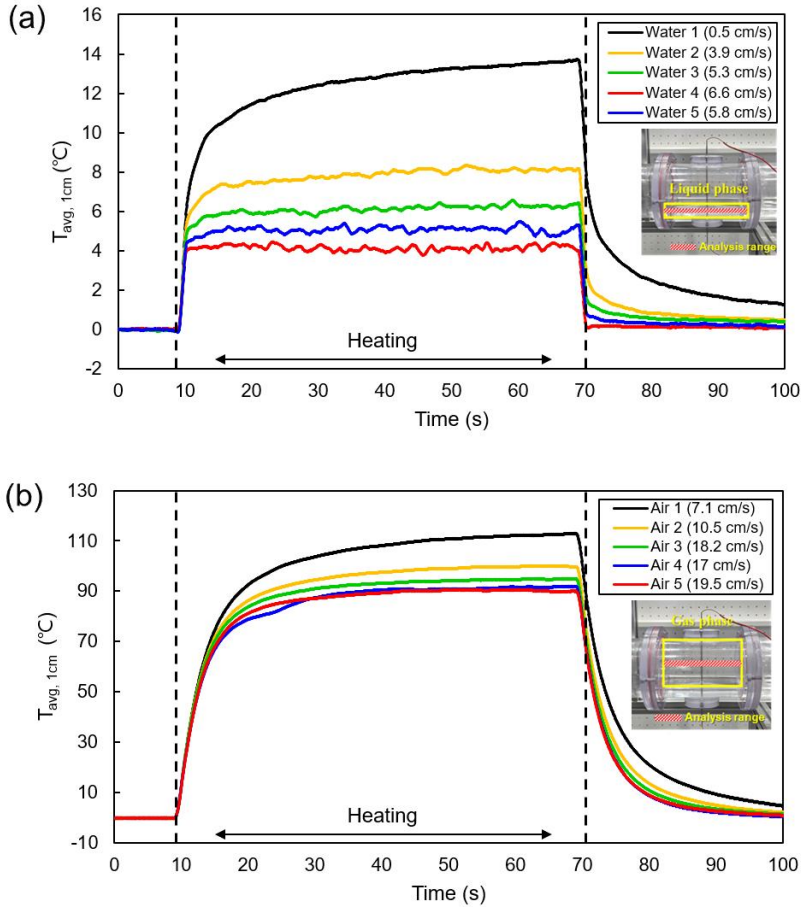

Figure 6: Time-series profiles of spatial-average temperature change at the center of each phase (a)liquid, (b)gas

Table 2: Inlet temperature fluctuation of all cases

No.	Fluctuation [℃]	No.	Fluctuation [℃]
Water 1	0.103	Air 1	0.119
Water 2	0.075	Air 2	0.122
Water 3	0.103	Air 3	0.138
Water 4	0.231	Air 4	0.512
Water 5	0.111	Air 5	0.163

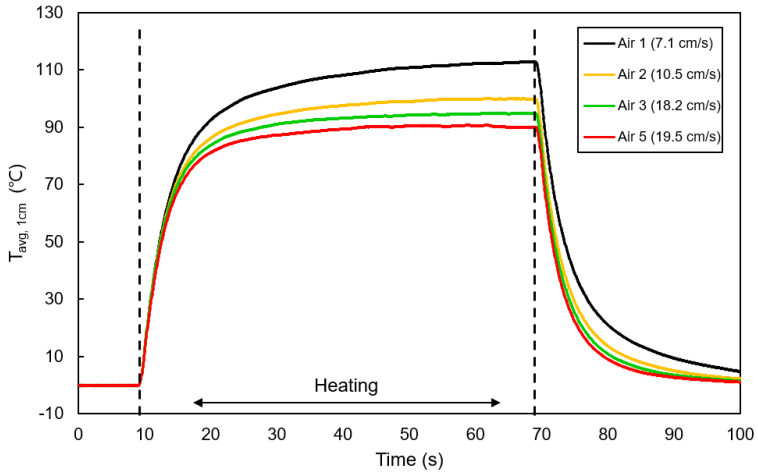

Figure 7: Refined gas phase thermal response profiles after filtering for thermal stability (fluctuation < 0.2 °C)

4 CONCLUSION

This study proposed and experimentally validated a technique for quantifying individual phase flow rates in an air-water stratified flow environment using a distributed fiber optic sensor. By achieving a high spatial resolution of 0.65 mm, the system obtained comprehensive cross-sectional flow information in real-time, which has been difficult to capture with conventional point-based sensors. The experimental results demonstrated that the inflection point in the temperature gradient, caused by differences in thermodynamic properties, coincided with the observed interface, thereby validating the estimation of the cross-sectional area. Furthermore, based on the principle of convective heat transfer, a clear inverse relationship was established where higher flow velocities resulted in lower quasi-equilibrium temperatures, providing a robust physical basis for velocity estimation. Under the current experimental conditions, a constant heat flux of 25 kW/m² was applied to both phases, however, the gas phase exhibited relatively high quasi-equilibrium temperatures due to its low heat capacity. Future research will focus on optimizing the heat flux to enhance sensor sensitivity by identifying a lower flux level that still induces a sufficient thermal response in the liquid phase. Additionally, further quantitative analysis will be conducted to determine the specific heating duration required for effective flow velocity discrimination, aiming to enhance the practical applicability and measurement precision of the proposed technique.

REFERENCES

[1] Mengyo W., Bo W., Xin G., Jiayi Z., Zhiyang C., Yang W., Chuan Lu., Yang W., Ruifeng T., Review on the steam-liquid separation in the steam generator of nuclear power plants, Annals of Nuclear Energy, Vol. 175, 109207, 2002.

[2] Hu C., Yu L., Wang D., He H., Li Y., Gas-liquid two-phase flow measurement by using electrical tomography sensors and Venturi, *Flow Measurement and Instrumentation*, Vol. 102, 102763, 2025

[3] Rivetti A., Martini G., Birello G., LHe venturi flowmeters: Practical design criteria and calibration method, *Cryogenics*, Vol. 34, No. 1, pp. 449-452, 1994.

[4] Wang H., Peng M., Wu P., Cheng S., Improved methods of online monitoring and prediction in condensate and feed water system of nuclear power plant, *Annals of Nuclear Energy*, 2016, 90: 44-53, 2016.

[5] Arief H.A., Wikotrski T., Thomas P.J., A Survey on Distributed Fiber Optic Sensor Data Modelling Techniques and Machine Learning Algorithms for Multiphase Fluid Flow Estimation, *Sensors*, Vol. 21, 2801, 2021.

[6] Christian M. Petrie, Joel L McDuffee, Liquid level sensing for harsh environment applications using distributed fiber optic temperature measurements, *Sensors and Actuators A: Physical*, Vol. 282, pp. 114-123, 2018.

[7] Chi X., Wang X., Ke X., Optical Fiber-Based Continuous Liquid Level Sensor Based on Rayleigh Backscattering, *Micromachines*, Vol. 13, No.4, 633, 2022.

[8] S. Lomperski, C. Gerardi, W.D. Pointer, Fiber optic distributed temperature sensor mapping a jet-mixing flow fied, *Exp Fluids*, Vol. 56, 55, 2015.

[9] Sekine M., Furuya M., Development of Measurement Method for Temperature and Velocity Field with Optical Fiber Sensor, *Sensors*, Vol. 23, 1627, 2023.

[10] Palmieri L., Schenato L., Distributed Optical Fiber Sensing Based on Rayleigh Scattering, *The Open Optics Journal*, Vol. 7, pp. 104-127, 2013.

[11] Brian J. Soller, Dawn K, Matthew S. Wolfe, Mark E. Froggatt, High resolution optical frequency domain reflectometry for characterization of components and assemblies, *Optics express*, Vol. 13, No. 2, pp. 666-674, 2005.

[12] Alex K. Sang, Mark E. Froggatt, Dawn K. Gifford, Stephen T. Kreger, Bryan D. Dickerson, One Centimeter Spatial Resolution Temperature Measurements in a Nuclear Reactor Using Rayleigh Scatter in Optical Fiber, *IEEE Sensors journal*, Vol. 8, No. 7, pp. 1375-1380, 2008.

[13] W. Sorin and D. Baney, Measurement of Rayleigh backscatter at 1.55μm with 32μm spatial resolution, *IEEE Photon. Technol. Lett.*, Vol. 4, pp. 374-376, 1992.

[14] M. Froggatt, J. Moore, High resolution strain measurement in optical fiber with Rayleigh scatter, *Appl. Opt.*, Vol. 37, pp. 1735-1740, 1998.

[15] Brain Culshaw, Alan Kersey, Fiber-Optic Sensing: A Historical Perspective, *Journal of lightwave technology*, Vol. 26, No. 9, pp. 1064-1078, 2008.

[16] Lu P., Lalam N., Badar M., Liu B., Chorpening B., Buric M., Ohodnicki P., Distributed optical fiber sensing: Review and perspective, *Appl. Phys.*, Vol. 6, No. 4, pp. 1-83, 2019.

ACKNOWLEDGEMENTS

This work was supported by the National Research Foundation of Korea (NRF) grant funded by the Korea government (Ministry of Science and ICT) (No. RS-2025-25445840), by the Korea Institute of Energy Technology Evaluation and Planning (KETEP) and the Ministry of Climate, Energy & Environment (MCEE) of the Republic of Korea (No. RS-2024-00398425), and by the Glocal University 30 Project fund of Gyeongsang National University in 2026.